SMALL-ANGLE NEUTRON SCATTERING CHARACTERIZATION OF GRAPHENE/Al NANOCOMPOSITES

X. M. DU[a,*], H. T. QI[a], T. F. LI[b], D. F. CHEN[b], Y. T. LIU[b], T. ZHAO[a], F. G. LIU[a], K. SUN[b], Z. J. WANG[b], D.CLEMENS[c], R. D. LIU[b], L.ZhANG[b], B. KENT[c]
[a]*School of Materials Science and Engineering, Shenyang Ligong University, Shenyang 110159, People's Republic of China*
[b]*China Institute of Atomic Energy, Beijing, 102413, People's Republic of China*
[c]*Helmholtz-Zentrum Berlin fürMaterialien und Energie, Lise-Meitner-Campus, Berlin, 14109, Germany*

The results of a Small-Angle Neutron Scattering (SANS) study are presented, aimed at the investigation of structural and morphological characteristics of graphene sheets in hot pressed graphene/Al nanocomposites. SANS gives an average conformation of graphene sheets in the nanocomposites, and scattering upon length scales from 125nm down to approximately 1 nm indicates scattering from local agglomerates of graphene sheets with mass fractal dimension changing from 1.4 to 1.9, and local structure of surfaces with the fractal dimension changing from 2.8 to 2.1. The diameter of local structure of graphene sheets that consists of plate-like objects, mostly containing folded, crumpled, aggregated sheets, is about 76 nm. These findings open up a new perspective in characterizing two-dimension materials as nano-scale reinforcing phases in composites using small-angle scattering techniques.

(Received November 3, 2018; Accepted April 13, 2019)

Keywords: SANS, Graphene, Aluminum matrix composites

1. Introduction

The development of high performance aluminum matrix nanocomposites by the incorporation of nanoparticles of different dimensions into aluminum matrices is of significant interest for next-generation advanced metallic materials. The prospect of achieving enhanced material properties such as light-weight, high strength, stiffness and resistance to high temperature by the addition of a small amount of nanoparticles has motivated a vast body of research [1-4]. In such materials, anisotropic nanoparticles like graphene or expanded graphite are becoming increasingly attractive due to their potential structural and functional applications in automotive, aerospace and military and general applications [5-7].

Among all expanded graphitic forms, graphene has fascinated by its unique strength and properties in the last few years. Graphene is endowed with excellent physical and mechanical properties such as tensile strength 130 (GPa), elastic modulus (0.5-1TPa) and thermal conductivity (5.3×10^3 $Wm^{-1}K^{-1}$) and has gotten attention in the field of research [8]. Graphene has been predictable to outperform due to its unique properties. Graphene have great potential in developing the nanocomposites when it is incorporated into matrix materials. A lot of research work has been conducted on the fabrication of aluminum composites based on reinforcing with graphene nanosheets [5,6,9], graphene nanoflakes [9-11], few-layered graphene [12], or its derivatives graphene oxide and reduced graphene oxide [13,14], and the mechanical properties of the composites can be significantly improved by addition of graphene. But it is still a great challenge to evaluate the extent of graphene dispersion in aluminum matrix composites by conventional characterization techniques, such as Scanning Electron Microscopy (SEM), Transmission Electron Microscopy (TEM) and Atomic Force Microscopy (AFM) etc. Despite offering dual advantages of obtaining very high resolution topographic images and compositional maps of the elements present in the matrix, the techniques suffer from a common drawback of analyzing a

*Corresponding author. du511@163.com.

highly localized portion compared to the entire bulk volume of the nanocomposite.

Small angle scattering techniques [15], such as small angle X-ray scattering (SAXS) and small angle neutron scattering (SANS), are capable to give information on the structural features of particles of colloidal size, as well as their spatial correlation. Both SAXS and SANS are powerful techniques for determining size, shape, and internal structure of particles in the size range from few nanometers up to about hundred nanometers. They give more reliable results from a statistical point of view, as the investigated area is of the order of some mm^2, against some hundreds of μm^2 (at maximum) in electron microscopy. In the past twenty years, researchers have reported the analysis of nano-reinforcement dispersion in polymer matrix nanocomposites [16-18] and ceramic matrix nanocomposites [19,20] from SAXS and SANS. Recently, the studies on size, morphological characteristics and dispersion of nano-scale graphene in polymer composites by SAXS and SANS have also been reported [21,22]. However, the reports on the dispersion of nano-scale graphene in metal matrix are scarce.

In the present work, the investigation of dispersion of nano-scale graphene was performed on the graphene/Al composite using the Small-Angle Neutron Scattering (SANS) technique. Though this method can be considered to be complementary to electron microscopy.The analysis of the SANS curves allowed the determination of the size and distribution of graphene.

2. Experimental procedures

2.1.Materials

Graphene sheets used in our experiments were prepared by modified hummers method as reported previously [23]. The graphene sheets with the thickness of 3-10 nm and the diameter of 5 μm were obtained. The preparation method was described in detail Ref. [24]. Atomized pure aluminum powder (AnShan Steel Industrial Fine Aluminum, Inc., Liaoning, China) with an average size of 20 μm and chemical composition (Fe 0.071 wt.%, Si 0.067 wt.%, Cu 0.002 wt.%) was used as matrix material.

2.2. Preparation of graphene/Al composites

Pure aluminum powders were initially mixed with 0.25, 0.5, 0.75, 1.0 wt.% as-prepared graphene sheets in a conventional rotating ball milling machine using the stainless jar and balls. Ball milling was carried out in argon atmosphere at a rotating speed of 50 rpm from 12 h to 48 hours with ball-to-powder weight ratio of 7:1. The designed graphene/aluminum composite samples is shown in Table 1. The above prepared graphene/Al powders were loaded into a heat-resistant steel die with a diameter of 50 mm. A sheet of graphitic paper was placed between the punch and the powders as well as between the die and the powders for easy removal. The compact graphene/Al composite billets were vacuum hot pressed at 605℃ for 1.5 hours under a pressure of 25 MPa by powder metallurgy. The graphene/Al composites were rolled at 520℃ with thickness reduction of 20-30% one pass. We prepared six samples as shown in Table 1.

Table 1.The graphene/aluminum composite samples.

Sample	Content of graphene wt.%	Ball milling time / h
Al1	0.25	12
Al2	0.25	24
Al3	0.25	48
Al4	0.5	48
Al5	0.75	48
Al6	1.0	48

2.3. SANS measurements

The SANS measurements were performed on the V16 SANS instrument at BERII research reactor HZB [25].To cover a wide scattering vector magnitude (q) range, two sample-to-detector distances were chosen, 2 and 11 m and the *q* range covered was therefore about 0.005-0.07$Å^{-1}$ and

0.06-0.6Å^{-1}, respectively. The neutron wavelength range of selected was λ = 0.28-0.9 nm with△ λ/λ= 0.01. The scattering background have been subtracted, by taking into account of the sample transmission. And then the two dimensional scattering data were reduced into the one dimensional I(q) (intensity versus the scattering vector magnitude) data format for further analysis.

3. Results and discussion

Fig. 1 shows the representative morphology of graphene. Graphene have a two-dimensional high aspect ratio sheet geometry, and the wrinkles and folds is also showed on the exfoliated graphene sheet, as depicted in Fig. 1. The graphene consisted of platelets with the morphology of irregular shaped flakes with mean diameters less than 5 um. The thickness of the graphene sheets was several nanometers (3-10 nm), corresponding to approximately 10-25 sheets of graphene (assuming that the thickness of monolayer graphene is 0.35nm [26]).

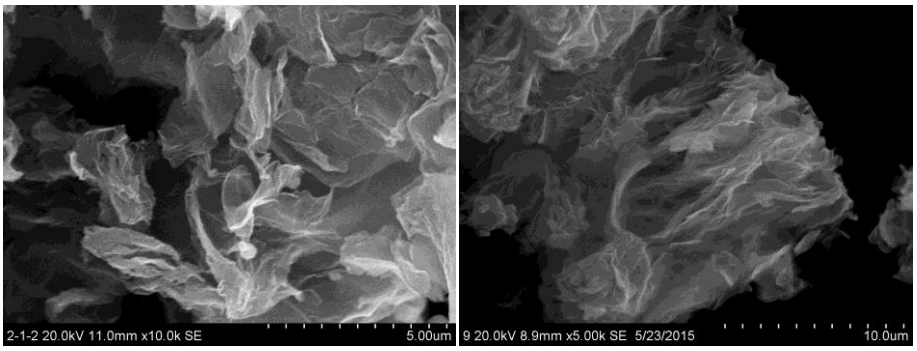

a) *b)*

Fig. 1.SEM images depicting the morphology of the graphene sheet.

SANS is potentially a very powerful technique for probing the structure and morphology of graphene in nanocomposites, as has been demonstrated for example by studies of polymer nanocomposites [21,27]. Specifically, SANS can be used to determine whether the graphene is present as single-layer or more agglomerated species as well as the graphene morphology (e.g., flat, rippled, or folded) [21,22]. Fig. 2 shows the SANS curves for the six graphene/aluminum composite samples. All samples demonstrate similar features, in particular those of mass fractal aggregates. As seen from Fig. 2, a double-logarithmic plot of I vs q power law scattering of the form q^{-p} coming from self-similar structures appears as a linear region of gradient -p, with the a exponent providing information on the dimensionality of the scatters. This exponent can also be a non-integer for disordered systems. In the disordered case the non-integer fractal dimension of the systemis given by $D= p$, for $p\in(1,3)$, or $D= 6-p$, for $p\in(3,4)$ in thecase of surface fractal behavior [28]. Generally, a power law of q^{-4} is indicative of a smooth surface, while between q^{-3} and q^{-4} is indicative of fractal surfaces with self-similar roughness. Power law exponents p extracted from least-squares fits to the data over the q-regions shown in Fig. 2 are listed in Table 2. From low q to high q (from left to right) the scattering features in Fig. 2 are as follows:

(a) The mass fractal scattering power law occurs at low q, ~0.005<q<~0.009Å^{-1} (probing length scales of 125 to 70 nm). This power law, corresponding to long length scales, shows sample-dependent variation, with -1.9<p1<-1.4. As shown in Fig. 2 (a), (b) and Table 2, the power law exponent p1 in this region variesas a function of ball-milling time and graphene concentration. This indicates that p1 values (Table 2) that yield the mass fractal dimension larger than -1.9 may result from local agglomerates of graphene sheets in composites. Based on the experience of SANS measurements on graphene sheets (or platelets) dispersions in solutions and polymers, it is known that slope values near to -2, are characteristic to a thin, two-dimensional sheet[21]. In order to support our findings we have also performed SEM measurements on facturesurfaces of the investigated graphene composites.The SEM image in Fig. 3 (a) clearly shows the presence of graphene agglomerates in the aluminum matrix, in agreement with the conclusions of the neutron scattering experiments. In Fig. 3 (b) a higher resolution image reveals that the agglomerates indeed

consist of multilayer graphene sheets.

(b) The Porod power law appears at high q, $0.02<q<0.2$ Å^{-1} (probing length scales of 30 to 3 nm). For all samples, the high q power law region has an exponent of $-3.9 \leq p2 \leq -3.2$, which corresponds to scattering by a surface fractal with $2.1 \leq D_s \leq 2.8$ [28]. We attribute this surface fractal behavior to the presence of the slightly roughened surface of graphene sheets. These D_s values are in agreement withthe ones obtained from the result that the dispersions containing scrolled or folded graphene platelets insolution are usually dominated by surface fractals, typically with D = 2-3 [27].

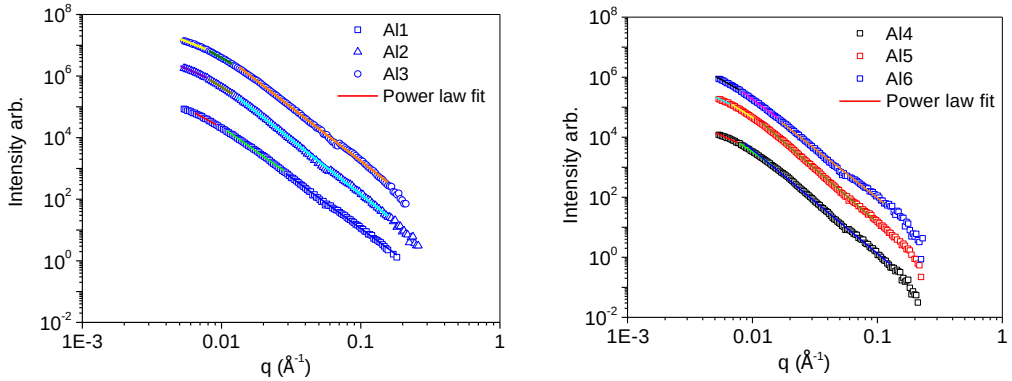

Fig.2. SANS data for the six composite samples plotted as I(q) vs q on log-log scales. For clarity the curves are offset by powers of 10 at q= 0.01 Å^{-1}. The solid lines are least-squares fits to a power law equation, I(q) -q^{p}. The power laws extracted from the fits are shown in Table 2.

Table 2. Exponents from power law fits to I(q) vs q SANS data shown in Fig.1.

Sample	low q exponent, *p1*	high-q exponent, *p2*	$D_s = 6 + p2$	q_c (Å^{-1})
Al1	-1.7	-3.2	2.8	0.010
Al2	-1.8	-3.7	2.3	0.009
Al3	-1.9	-3.5	2.5	0.008
Al4	-1.7	-3.8	2.2	0.009
Al5	-1.6	-3.7	2.3	0.009
Al6	-1.4	-3.9	2.1	0.009

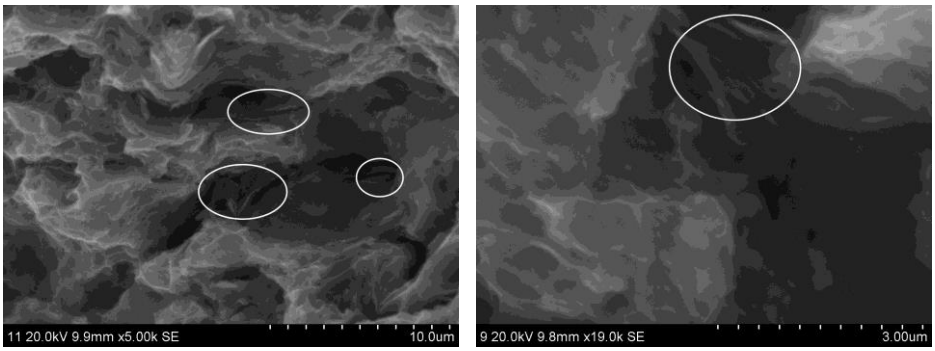

a) *b)*

Fig. 3. Scanning electron micrographs of aluminum composite fracture surfaces reinforced with graphene sheets: (a) showing the presence of graphene agglomerates, marked by white ellipses. (b) Revealing that the agglomerates consist of multilayer graphene sheets.

All of the composite samples demonstrate power law Porod regions with no fluctuation. Under the circumstances, it is difficult to identify a specific q value corresponding to the primary particle size in the $I(q)$ vs q data, Fig. 2. It is tempting to locate the crossover at the intersection of the mass fractal and Porod power laws. However, the derivative of the experimental SANS curves, Fig. 4, indicates that there is an obvious dividing point between the mass fractal region and the surface fractal region. The derivative method directly shows a crossover value q_c between the two regimes. It means that q_c is also identical to the low q limit of the linear fit to the Porod regime in $I(q)$ vs q data.Table 2 shows the derivative determined value of q_c for all composites. The values of q_c are in range of 0.008-0.01 $Å^{-1}$ which corresponds to the beginning of the domain where $q^{-p2}I(q)$ remains constant (for broad particle size distributions).

In comparison with the SANS measurement window (125 to 3 nm in this case), the graphene used in this study has a large lateral size of approximately 5 μm. This means that even with a large degree of folding, the scattering upon the length scales probed is primarily from the local structure, e.g., the nature of the surfaces present, rather than being able to resolve scattering from entire graphene objects. In order to characterize larger features by neutron scattering ultra-small angle scattering experiments have to be performed.

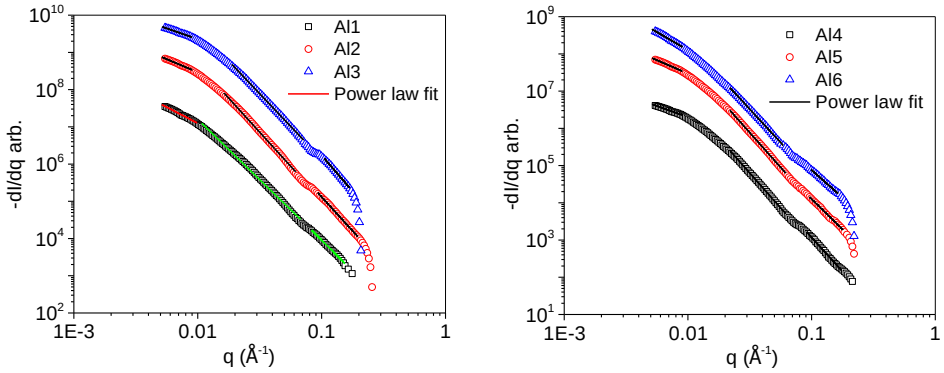

Fig. 4. Plots of-dI/dq vs q for the six aluminum matrix composites. The derivative is calculated from successive points in I(q) vs q data Fig.2, as△I/△q. The derivative is plotted against the midpoint of successive q values. The solid lines are least-squares fits to a power-law equation. The crossover point between surface scattering of the primary particles and scattering by the mass fractal is taken as the intersection of the two power laws; see Table 2.

For extremely dilute and monodispersed systems, the Guinier approximation allows the determination of the particle size from the radius of gyration r_g [29, 30] from the slope in a diagram of the logarithmic intensity vs. the square of the scattering vector towards small q. However, Guinier approximation should not be applicable here, considering the complex structure of the system, and the limited measured q-range. Guinier approximation is in practice applied to dilute sets of polydisperse nano-objects only when the size distribution has a moderate width. For very polydisperse systems, the q-range over which Guinier approximation holds is very small. On the other hand, Guinier plots yield in this case an average radius of gyration far from the arithmetic average and strongly biased towards those of the biggest objects [31]. Anyway it is not always easy to establish exactly the q-range in which this linearity holds, and significantly different r_g values can be obtained by choosing different q-ranges to this end. Therefore, an alternate method can be used to calculate r_g, that is by plotting the function $q^2I(q)$ vs. q, which has a maximum at $q = \sqrt{3} / r_g$.

Fig. 5 shows the plots of $q^2I(q)$ vs. q for the six investigated composites. The q value corresponding to maximum position of the plots of $q^2I(q)$ vs. q for all composites is 0.006416$Å^{-1}$. The value of the gyration radius r_g, of the six investigated composites is 270 Å which indicates a constant in the graphene sheet size, independent of the content of graphene. In the case of platelets ($h<<R$, where h is the platelet thickness and R is the platelet radius), the relationship between the geometric radius, R of a thin disk shaped particle and its gyration radius r_g is $r_g = R / \sqrt{2}$ [30]. According to this relationship, the diameter of graphene sheets in six investigated composites is about 76 nm which is more less than 5 μm. In present SANS measurement window, the q range

covered is about 0.005-0.6Å $^{-1}$ in which probing length scales is from 125 to 1 nm. Therefore the scattering from the local graphene structure within the aluminum matrix composite is dominated from length scales of 125 nm and below.Weir et al.[21] confirmed the presence of the local graphene oxide structure with folded, crumpled, or aggregated sheets in polymer−graphene oxide nanocomposites by SANS of measurement window of approximately~100 nm.

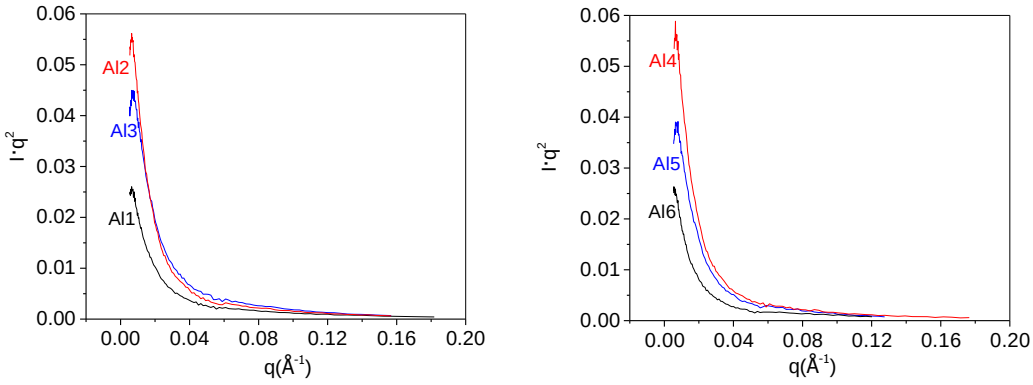

Fig. 5. SANS $q^2I(q)$ vs. q plots for the six investigated composites.

4. Conclusions

The Small-Angle Neutron Scattering technique was successfully applied to the study of the microstructure of graphene/Al nanocomposites, obtained by a ball-milling method followed by hot pressed sintering. In particular, the size of the graphene sheets and its fractal behavior were determined, independent of graphene content. SANS gives an average conformation of graphene sheets in the nanocomposites, and scattering upon length scales from 125 nm down to approximately 1 nm indicates scattering from local agglomerates of graphene sheets with mass fractal dimension changing from 1.4 to 1.9, and local structure of surfaces with the fractal dimension changing from 2.8 to 2.1. The crossover point at the intersection of the mass fractal and Porod power laws can be determined from experimental small-angle scattering data by plotting -dI/dq vs q. Furthermore, the diameter of local structure of graphene sheets that consists of plate-like objects, mostly containing folded, crumpled, aggregated sheets is about 76 nm. This study opens up the possibility of studying the local structure of two-dimensional materials using small-angle scattering techniques.

Acknowledgements

This work was supported by Shenyang Science and Technology Project (No.18-013-0-33), Shenyang Young and Middle-aged Science and Technology Innovation Talents Project (RC180214) in Liaoning Province, China and the National Science Foundation of China (No.11575295). We thank HZB for the allocation of neutron beamtime.

References

[1] L. Kollo, C. R. Bradbury, R. Veinthal, C. Jaggi, E. Carreno-Morelli, M. Leparoux, Mater.Sci. Eng. A **528**, 6606 (2011).
[2] H. G. Prashantha Kumar M. A.Xavior, Tribology – Materials, Surfaces & Interfaces, 1(2017).
[3] S. C. Tjong, Mater. Sci. Eng. R **74**, 281 (2013).
[4] R. P. Bustamante, F. P. Bustamante, I. E. Guel, L. L. Jiménez, M. M. Yoshida, R. M. Sánchez, Mater. Charact.**75**, 13 (2013).
[5] S. F. Bartolucci, J. Paras, M. A. Rafiee, J. Rafiee, S. Lee, D. Kapoor, Mater.Sci. Eng. A **528**,

7933 (2011).
[6] A. F. Boostani, S. Tahamtan, Z. Y. Jiang, D. Wei, S. Yazdani, R. A. Khosroshahi, R. T. Mousavian, J. Xu, X. Zhang, D. Gong, Composites: Part A **68**, 155 (2015).
[7] K. Markandan, J. K. Chin, J. Mater. Res. **32**, 84 (2017).
[8] H. G. P. Kumar, M. A. Xavior, Procedia Eng. **97**, 1033 (2014).
[9] S. J. Yan, Y. Cheng, H. Q. Hu, C. J. Zhou, L. D. Bo, D. S. Long, J. Mater. Eng. **4**, 1 (2014).
[10] J. L. Li, Y. C. Xiong, X. D. Wang, S. J. Yan, C. Yang, W. W. He,J. Z. Chen, S. Q. Wang, X. Y. Zhang, S. L. Dai, Mater.Sci. Eng. A **626**, 400 (2015).
[11] M. Rashad, F. Pan, A. Tang, M. Asif, Progress in Natural Science: Materials International **24**, 101 (2014).
[12] S. E. Shin, H. J. Choi, J. H. Shin, D. H. Bae, Carbon **82**, 143 (2015).
[13] Z. Li, G. Fan, Z. Tan, Q. Guo, D. Xiong, Y. Su, Z. Q. Li, D. Zhang,Nanotechnology**25**, 325601 (2014).
[14] J. Wang, Z. Li, G. Fan, H. Pan, Z. Chen, D. Zhang, Scripta Materialia **66**, 594 (2012).
[15] Y. Leng, Materials Characterization: Introduction to Microscopic and Spectroscopic Methods; John Wiley & Sons, Ltd.: Singapore, 2008.
[16] P. Akcora, S. K. Kumar, J. Moll, S. Lewis, L. S. Schadler, Y. Li, B. C. Benicewicz, A. Sandy, S. Narayanan, J. Ilavsky, Macromolecules **43**, 1003 (2010).
[17] M. García-Gutiérrez, A. N. Ruiz, Opt. Pura Y. Appl.**40**, 195 (2007).
[18] A. A. Golosova, J. Adelsberger, A. Sepe, M. A. Niedermeier, P. Lindner, S. S. Funari, R. Jordan, C. M. Papadakis, J. Phys. Chem. C**116**,15765 (2012).
[19] M. Ohnuma, K. Hono, H. Onodera, S. Ohnuma, H. Fujimori, J. S. Pedersen, J. Appl. Phys.**87**, 817 (2000).
[20] S. Hazra, A. Gibaud, A. Desert, Phys. B**283**, 97 (2000).
[21] M. P. Weir, D. W. Johnson, S. C. Boothroyd, R. C. Savage, R. L. Thompson, S. R. Parnell, A. J. Parnell, S. M. King, S. E. Rogers, K. S. Coleman, N. Clarke, Chem. Mater. **28**, 1698 (2016).
[22] T. Mondal, R. Ashkar, P. Butler, A. K. Bhowmick, R. Krishnamoorti, ACS Macro Lett. **5**, 278 (2016).
[23] W. S. Hummers, R. Offeman, J. Am. Chem. Soc. **80**, 13 (1958).
[24] X. M. Du, R. Q. Chen, F. G. Liu, Digest Journal of Nanomaterials and Biostructures **12**, 37 (2017).
[25]K. Vogtt, M. Siebenbürger, D. Clemens, C. Rabe, P. Lindner, M. Russina, M. Fromme, F. Mezei, M. Ballauff, J. Appl. Cryst.**47**, 237 (2014).
[26] W. Choi, I. Lahiri, R. Seelaboyina, Y. S. Kang,Crit. Rev. Solid State Mater. Sci. **35**, 52 (2010).
[27] E. M. Milner, N. T. Skipper,C. A. Howard, M. S. P. Shaffer,D. J. Buckley, K. A. Rahnejat, P. L. Cullen,R. K. Heenan, P. Lindner, R. Schweins, J. Am. Chem. Soc.**134**, 8302 (2012).
[28] D. W. Schaefer, R.S. Justice, Macromolecules **40**, 8501 (2007).
[29] A. Guinier, G. Fournet, Small-Angle Scattering of X-rays, Chapman & Hall, London, 1955.
[30] L. A. Feigin, D. I. Svergun, Structure Analysis by Small-Angle X-ray and Neutron Scattering, Plenum Press, New York, 1987.
[31] A. F. Craievich, Small-Angle X-ray Scattering by Nanostructured Materials. In: L. Klein, M. Aparicio, A. Jitianu (eds) Handbook of Sol-Gel Science and Technology. Springer, Cham, 1(2016).